Clays and Clay Minerals, Vol. 65, No. 5, 299–309, 2017.

OXIDATION AND CATALYTIC OXIDATION OF DISSOLVED SULFIDE BY MANGANITE IN AQUEOUS SYSTEMS

YAO LUO, SHAN LI, WENFENG TAN, GUOHONG QIU*, FAN LIU, AND CHONGFA CAI

Key Laboratory of Arable Land Conservation (Middle and Lower Reaches of Yangtse River), Ministry of Agriculture, College of Resources and Environment, Huazhong Agricultural University, Wuhan 430070, China

Abstract—As one of the strongest inorganic oxidizers in natural environments, manganese oxides participate in the oxidation processes of dissolved sulfides, affecting their migration, transformation, and toxicity. The amount of and sites for Mn(III) influence significantly the oxidation activity of Mn(IV) oxides. As an easily formed Mn oxide in supergene environments, manganite consists of $Mn(III)O_6$ octahedra; further study is needed of the interaction processes of manganite and dissolved sulfide. In the present study, the interaction mechanisms of dissolved sulfide and manganite were studied systematically. The influences of pH, temperature, and oxygen atmosphere were also investigated in detail. X-ray diffraction (XRD) and transmission electron microscopy (TEM) were used to characterize the crystal structures, compositions, and micromorphologies of manganite and the intermediate products. The sulfide species were identified by visible spectroscopy, high-performance liquid chromatography, UV-visible (UV-Vis) spectroscopy, and ion chromatography during the reaction process. The results indicated that in a nitrogen atmosphere, elemental sulfur was formed as the main oxidation product of dissolved sulfide by manganite at the initial stage, and polysulfide ions were observed as the intermediates. Elemental sulfur was further oxidized slowly to $S_2O_3^{2-}$. The initial oxidation rate of dissolved sulfide by manganite increased with temperature from 20 to 40ºC. The reaction rate increased at first and then decreased as the pH changed from 4.0 to 12.0, and the greatest oxidation rate was achieved at pH 8.0. In the presence of oxygen, $S_2O_3^{2-}$ was the main product. The oxidation rate of dissolved sulfide decreased, and manganite exhibited significant catalytic activity and stability with respect to the oxidation of dissolved sulfide in the oxygenated aqueous systems. These findings are of fundamental significance in understanding the interaction and transformation of dissolved sulfide and manganese oxides in nature.

Key Words—Catalysis, Dissolved Sulfide, Manganite, Redox Reaction, Soil Environment.

INTRODUCTION

As common metal (hydr)oxides in supergene environments, manganese oxides are distributed widely in soils and sediments, affecting the migration, transformation, and fate of toxic metal ions and organics, such as Cu, Pb, Zn, As, and desferrioxamine B (Walker and Hayes, 1990; Duckworth and Sposito, 2005; Toner *et al*., 2006; Mongelli *et al*., 2015). Manganite (γ-MnOOH) is the most stable and abundant low-valence manganese oxide mineral which can be formed by the abiotic oxidation of aqueous Mn(II) and the reduction of Mn(IV) oxides (Stumm and Giovanoli, 1976; Murray *et al*., 1985; Golden *et al*., 1987; Tu *et al*., 1994). The reduction of birnessite, cryptomelane, and todorokite and the oxidation of $Mn(OH)_2$ usually leads to the formation of metastable feitknechtite (β-MnOOH) (Stumm and Giovanoli, 1976; Tu *et al*., 1994; Qiu *et al*., 2011; Gao *et al*., 2015). Feitknechtite is usually generated as an intermediate and can be transformed further into manganite (Stumm and Giovanoli, 1976; Murray *et al*., 1985), *i.e.* manganite can be formed naturally in soil environments and affects the redox behavior of contaminants.

Dissolved sulfide shows high toxicity and corrosivity. The oxidation of sulfide causes soil acidification, acid mine drainage, and contaminant leaching. In natural environments, dissolved sulfide can be oxidized by microbes, oxygen, and active metal oxides including ferric oxides and manganese oxides (Rickard, 1974; Yao and Millero, 1993; Johnson and Hallberg, 2003). The oxidation activity of bacteria is affected remarkably by the acidity of environments. The oxidation of sulfide minerals by microorganisms usually occurs in extremely acidic environments (pH < 3) (Johnson and Hallberg, 2003). Chemical reactions are suggested to play an important role at the initial stage of the oxidation of sulfide in soil solutions.

As a group of the strongest inorganic oxidizers in the environment, manganese oxide minerals participate in the oxidation processes of dissolved sulfide and metal sulfides (Aller and Rude, 1988; Yao and Millero, 1993; Schippers and Jørgensen, 2001; Liu *et al*., 2009). The reaction mechanism and kinetics of sulfide oxidation by Mn(IV) oxides have been studied extensively. A previous study showed that the crystal structure and chemical composition of manganese oxides affect the process and kinetics of sulfide oxidation (Herszage and

* E-mail address of corresponding author:
qiugh@mail.hzau.edu.cn
DOI: 10.1346/CCMN.2017.064066

dos Santos Afonso, 2003). Mn(III) content is considered as a rate-controlling factor in sulfide oxidation by δ-MnO_2 (Nico and Zasoski, 2001). Previous results further revealed that Mn(III) sites play a more significant role than the type of crystal structure in improving the oxidation rate of dissolved sulfide (Qiu *et al*., 2011). In the reaction system of dissolved sulfide and todorokite, the decreased amount of Mn(III) in todorokite, due to the formation of Mn(IV) in the presence of oxygen, resulted in an increase in the chemical stability of todorokite and a decrease in the oxidation rate of dissolved sulfide at the initial stage (Gao *et al*., 2015). In comparison with cryptomelane, birnessite, and todorokite, manganite shows weaker oxidation activity and can be formed more easily in soil environments (Gao *et al*., 2015; Luo *et al*., 2017). The transformation process of Mn(III) is worth studying when manganite participates in the oxidation reaction of dissolved sulfide. The reaction rate of dissolved sulfide and manganite is not affected appreciably by initial pH, which would increase rapidly as the reaction proceeds (Luo *et al*., 2016), but the dependence of the reaction mechanism on pH remains elusive. In the above experiments, intermediate products were only characterized within a short time, and further transformation processes are still unknown. A systematic study of the environmental chemical behaviors between manganite and dissolved sulfide is needed.

In natural environments, the concentration of dissolved oxygen in some micro systems is greater than that in general aqueous systems such as rhizosphere soils (Li *et al*., 2011; Zhang *et al*., 2012; Shamsul Haque *et al*., 2015). A high concentration of dissolved oxygen and manganese oxides can co-participate in the oxidation of dissolved sulfide in aqueous environments. Todorokite works as a catalyst during the oxidation of dissolved sulfide by oxygen at the initial stage, and it is slowly reduced to $Mn(OH)_2$ at the later stage (Gao *et al*., 2015), which can be further oxidized to manganite by oxygen. Hence, the redox processes of dissolved sulfide and manganite in the presence of oxygen are worthy of further investigation.

The objective of the present study was to increase understanding of the redox and transformation processes of dissolved sulfide and manganite in natural systems, and to elucidate the influences of pH, temperature, and the presence of oxygen on the reaction processes and kinetics of dissolved sulfide and manganite.

MATERIALS AND METHODS

Chemicals

The NaOH, $MnSO_4{\cdot}H_2O$, H_2O_2 (30%), $Na_2S{\cdot}9H_2O$, $NaCH_3COO{\cdot}3H_2O$, KI, I_2, $Zn(CH_3COO)_2{\cdot}2H_2O$, $NH_3{\cdot}H_2O$, *N,N*-dimethylphenylenediamine, $Fe(NH_4)(SO_4)_2{\cdot}12H_2O$, $Na_2S_2O_3$, $K_2Cr_2O_7$, $AgNO_3$, CH_3OH, and soluble starch used were all of reagent grade and purchased from China National Medicine Group, Shanghai Chemical Reagent Company (Shanghai, China). Distilled deionized water (DDW, 18 MΩ cm, from Labconco WaterPro Ps, Kansas City, Kansas, USA) was boiled for 1 h to remove the dissolved oxygen and then cooled to room temperature with continuously bubbling nitrogen to remove the residual dissolved oxygen. Deoxygenated DDW was sealed with cling film before use in the redox experiments. All glassware and polyethylene centrifuge tubes were rinsed with 0.01 mol L^{-1} HNO_3 solution and DDW before use.

Redox experiments

Manganite was synthesized with the oxidation of $MnSO_4$ by H_2O_2 in alkaline solution (Giovanoli and Leuenberger, 1969). The as-obtained sample was dried in an oven at 40ºC and ground in an agate mortar to pass through a 75-mesh sieve. The synthesized manganite was characterized by powder XRD and was indexed on the monoclinic unit cell for γ-MnOOH (JCPDS card ID: 41-1379). The average oxidation state of manganese was established as 3.02, further suggesting that highly pure-phase manganite was obtained. The structure and chemical composition of synthesized manganite under experimental conditions were similar to those of natural manganite (Weaver e*t al*., 2002). The Brunauer-Emmer-Teller (BET) surface area was determined to be 42.4 m^2 g^{-1}, which was larger than that of naturally occurring manganite (Weaver e*t al*., 2002).

All solutions in redox experiments were prepared using deoxygenated DDW. 600 mg of $Na_2S{\cdot}9H_2O$ was dissolved into 400 mL of deoxygenated DDW, and the concentration of dissolved sulfide (HS^-) was ~200 mg L^{-1} (6.25 mmol L^{-1}) without adjusting the pH, which was ~12.0. This selected concentration was close to that of dissolved sulfide in wastewater from petrochemical industries (Xu *et al*., 2014) which will lead to the pollution of surrounding soils. Na_2S aqueous solution was first adjusted to the predetermined pH by dropwise addition of HCl (0.1 and 1.0 mol L^{-1}) and NaOH (0.1 mol L^{-1}) solutions. The pH of the reaction system of dissolved sulfide and manganite (1.25 g L^{-1}) was further controlled by manual addition of HCl and NaOH solutions during the redox processes. When the pH was controlled at between 4.0 and 10.0, an automatic potentiometric titrator (Metrohm 907, Titrando, Herisau, Switzerland) was used to adjust pH in the first 12 h and the pH was then controlled by manual addition of HCl and NaOH solutions. To reduce the effect of the volume of acid/base titration solution on the concentration of the reactant in the reaction system at lower pH, a greater concentration (1.0 mol L^{-1}) of HCl solution was used in the first 12 h. The reaction temperature was controlled variously at 20, 30, and 40ºC before the addition of manganite, and was fixed in reaction processes using a constant-temperature oil bath. To determine the possible intermediates, 0.625 g L^{-1} of manganite was used in the

https://doi.org/10.1346/CCMN.2017.064066 Published online by Cambridge University Press

experiment to decrease the reaction rate and accelerate the formation of polysulfide.

A 500 mL, five-mouth columnar flask was used as the reactor, which was bubbled continuously with high-purity nitrogen gas (99.999%, Wuhan Iron and Steel (Group) Corp., Wuhan, China) from a high-pressure vessel with an initial pressure of 15 MPa. Nitrogen pressure inside the reactor was kept slightly higher than atmospheric pressure to prevent air ingress. To study the transformation process of dissolved sulfide in oxygenated environments, pure oxygen (99.9%, Wuhan Iron and Steel (Group) Corp.) rather than nitrogen was pumped continuously into the solution to allow the dissolution of sufficient oxygen in the reaction system.

Product characterization

The synthesized manganite was characterized by XRD (Bruker D8 Advance, Bruker, Karlsruhe, Germany) using CuKα radiation (λ = 0.15406 nm) equipped with a LynxEye detector. The diffractometer was operated with a tube voltage of 40 kV and a tube current of 40 mA at a scanning rate of 4º2θ min^{-1}. The average oxidation state was measured by an oxalic method (Hem, 1981), and the BET surface area of the product was measured using a Micromeritics ASAP 2020 automated N_2 gas adsorption system (Micromeritics, Norcross, Georgia, USA).

3 mL of suspending liquid in the reaction system was drawn and filtered through a cellulose acetate 0.22 μm microporous membrane filter (Shanghai Xinya Purification Material Factory, Shanghai, China) at different reaction times. The solid intermediates including manganese (hydr)oxides and elemental sulfur collected by filtration were determined by XRD. Transmission electron microscopy (TEM, Hitachi H-7650, Tokyo, Japan) was used to characterize the microstructures of manganite and the transformation products at 200 kV imaging on a holey carbon-coated copper grid. Elemental sulfur in a 3.0 mL reaction solution was filtered off, dissolved in methanol, and then filtered again and quantified by high-performance liquid chromatography using an Agilent 1200 instrument (Agilent, Beijing, China) with a UV-Vis detector at 254 nm (Möckel, 1984; Herszage and dos Santos Afonso, 2003). The samples were injected into a 50-μL loop and passed through an Eclipse XDB-C_{18} analytical chromatographic column, and the column temperature was maintained at 25ºC. A standard sample was prepared by dissolving powdered elemental sulfur in pure methanol, and the methanol solution containing 5% water was used as the eluent (Schippers *et al*., 1996; Herszage and dos Santos Afonso, 2003).

The dissolved sulfide concentration in the filtrate was determined by the methylene blue method using visible spectroscopy (721/SP-721, Shanghai King Tech Industry Co., Ltd., Shanghai, China), and the standard concentration of dissolved sulfide was demarcated by iodimetry and back-titration with a standard sodium thiosulfate solution (Caldwell and Krauskopf, 1929). Polysulfide ions were detected using UV-Vis spectroscopy (UV-6300PC double beam spectrophotometer, Shanghai Mapada Instruments Co., Ltd, Shanghai, China). The composition and concentration of SO_3^{2-}, $S_2O_3^{2-}$, and SO_4^{2-} were analyzed by ion chromatography (Dionex ICS-1100, California, USA) using a conductivity detector with a resolution of 0.003 nS cm^{-1}. The eluent was a 1.0 mmol L^{-1} Na_2CO_3/36.0 mmol L^{-1} of $NaHCO_3$ solution with a flow rate of 1.5 mL min^{-1}. The current was controlled at 142 mA and the column temperature was maintained at 30ºC. The transformation ratio from dissolved sulfides to intermediates was calculated as the ratio of the concentration of the oxidized sulfur species intermediate to that of the initial dissolved sulfide. Total S indicated the sum of the determined oxidized sulfide species including elemental S, $S_2O_3^{2-}$, SO_3^{2-}, and SO_4^{2-}. The concentration of dissolved Mn(II) in the filtrate was determined by atomic absorption spectrometry (Varian AA240FS, Palo Alto, California, USA). The redox experiments were conducted and repeated at least twice. All chemical analyses for each sample were repeated three times.

RESULTS AND DISCUSSION

Oxidation of dissolved sulfide by manganite in nitrogen atmosphere

The redox process of dissolved sulfide and manganite was studied in aqueous systems with pH 12.0 under nitrogen atmosphere for 30 days, and the concentrations of HS^-, elemental S, $S_2O_3^{2-}$, SO_3^{2-}, and SO_4^{2-} were analyzed at various times. The concentration of dissolved sulfide decreased rapidly over time at the initial stage and approached 39.58 mg L^{-1} after 1.0 h, *i.e.* ~80% of the sulfide was oxidized (Figure 1a). Compared with the previously used oxidants birnessite, cryptomelane, and todorokite, under similar conditions (Gao *et al*., 2015; Qiu *et al*., 2011), manganite showed less oxidation activity, as indicated by the much longer reaction time for the complete transformation of sulfide. The intermediate products of HS^- oxidation were further characterized by ion chromatography and spectrophotometry for various times (Figure 1b). The transformation ratio from HS^- to elemental S increased within the first 2 h, and then decreased to zero after 600 h. The transformation ratio from HS^- to $S_2O_3^{2-}$ increased and approached 94.3% after 720 h. The transformation ratio from HS^- to SO_3^{2-} and SO_4^{2-} was <4%. Elemental S was formed as the main intermediate at the beginning of the reaction and its concentration decreased in the later stage, attributed to further oxidation of elemental S by manganite and the interaction of S and SO_3^{2-} to form $S_2O_3^{2-}$ (Qiu *et al*., 2011; Gao *et al*., 2015). In previous studies, the transformation from HS^- to elemental S was studied only within the first several hours of reaction (Qiu *et al*., 2011; Gao *et al*., 2015; Luo *et al*., 2016), but

https://doi.org/10.1346/CCMN.2017.064066 Published online by Cambridge University Press

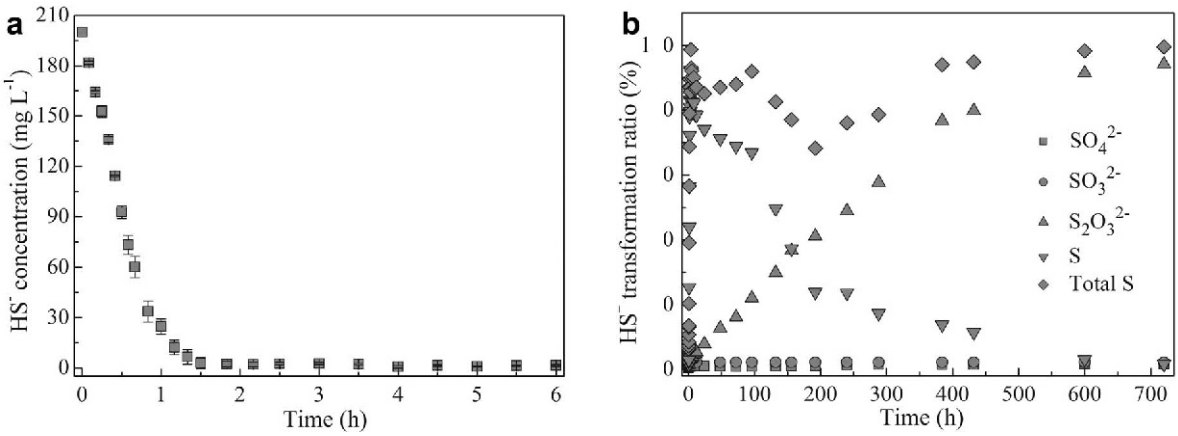

Figure 1. Concentration of HS^- (a) and transformation ratio from HS^- to intermediates (b) for the oxidation by γ-MnOOH (1.25 g L^{-1}) at different times in an aqueous system with pH 12.0 in a nitrogen atmosphere at 20ºC.

further transformation processes and final products were still unknown. In the present study the redox reaction lasted for 30 days in nitrogen atmosphere, and the elemental sulfur was oxidized completely to $S_2O_3^{2-}$.

The total transformation ratio from HS^- to elemental S, $S_2O_3^{2-}$, SO_3^{2-}, and SO_4^{2-} was <100% at the initial stage (Figure 1b). After 720 h of reaction, the total transformation ratio of dissolved sulfide approached ~100%, suggesting that the volatilization of dissolved sulfide could be negligible. The transformation ratio of total S was established as being <<100% within 100–300 h, however, indicating the existence of some other intermediates. Polysulfide ions, which could be generated by the interaction of elemental S and dissolved sulfide, were probably the important products in this reaction system. Polysulfide ions usually have significant reaction activity and an undefined degree of polymerization which were affected by the concentration of sulfides, elemental S, and H^+ (Lippa and Roberts, 2002; Kamyshny *et al*., 2004). They were seldom examined quantitatively *ex situ*, therefore, probably because of their rapid interactions and further oxidation by oxygen in air during sample-treatment processes (Yao and Millero, 1993; Schippers and Jørgensen, 2001). Birnessite, cryptomelane, and todorokite have strong oxidation capability and can oxidize polysulfide ions rapidly. Polysulfide ions may be oxidized to elemental sulfur and sulfate (Yao and Millero, 1993) and may also be decomposed thermally to hydrogen sulfide and thiosulfate ions (Filpponen *et al*., 2006).

Manganite exhibited weaker oxidation activity than birnessite, cryptomelane, and todorokite, facilitating the measurement of polysulfide ions during the reaction process. To examine the possibility of the existence of polysulfide ions in the oxidation of dissolved sulfide, a manganite concentration of 0.625 g L^{-1} was used to reduce the reaction rate and to avoid the further oxidation of polysulfide ions by excess manganese oxide. A yellow suspension was observed at the initial stage (Figure 2a), which was discolored after a period of time. The solid

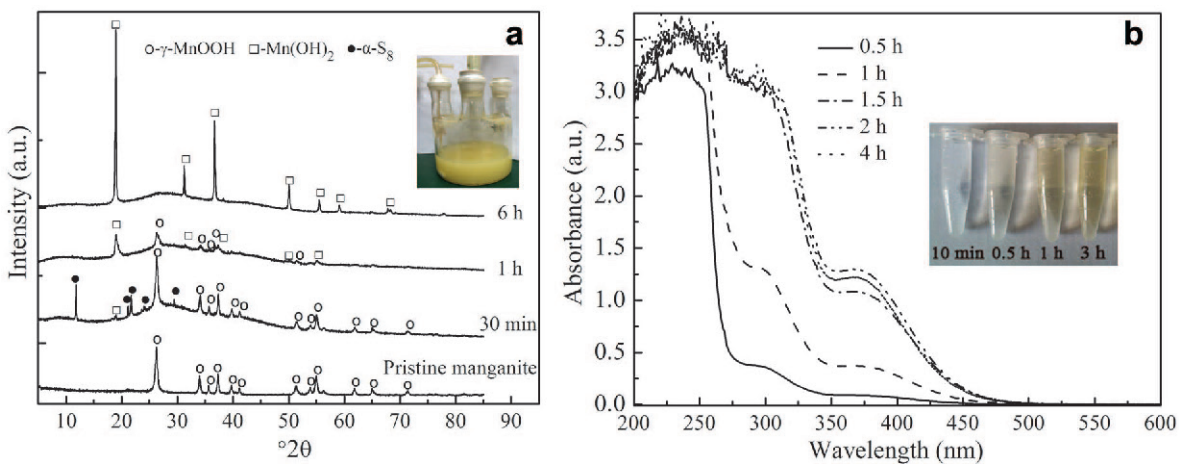

Figure 2. XRD patterns of solid products and photo of reaction system (a); UV-Vis spectra of aquatic products and filtrate photos (b) of HS^- (400 mL, 200 mg L^{-1}) and γ-MnOOH (0.625 g L^{-1}) with pH 12.0 at 20ºC in a nitrogen atmosphere.

https://doi.org/10.1346/CCMN.2017.064066 Published online by Cambridge University Press

products were characterized to be a mixture of γ-MnOOH, $Mn(OH)_2$ (JCPDS card ID: 12-0696), and α-S_8 (JCPDS card ID: 83-2284) after 30 min of reaction (Figure 2a). A mixture of $Mn(OH)_2$ and γ-MnOOH was formed after 1 h, and γ-MnOOH was consumed completely with the formation of $Mn(OH)_2$ as the main product after 6 h. These results indicated that α-S_8 was formed as an intermediate and was oxidized subsequently at the later stage. Images of the filtrate after various reaction times showed that colorless filtrate was observed after 10 min of reaction (Figure 2b). Yellow-white filtrate was formed after 30 min. It turned light yellow and deep yellow after 1 h and 3 h of reaction, respectively, suggesting that some aqueous intermediates were formed. The filtrate was analyzed by UV-Vis spectroscopy (Figure 2b). The absorption peak at ~370 nm was attributed to polysulfide ions including S_4^{2-} and S_5^{2-} (Hoffmann, 1977). The intensity of this absorption peak increased in the first 2 h and then decreased after 4 h (Figure 2b), indicating that polysulfide ions were formed as intermediates during the redox processes of dissolved sulfide and manganese oxides. Based on the discussion above, the redox mechanism of dissolved sulfide and manganite could be summarized as follows: $Mn(OH)_2$ and α-S_8 were formed as the main products at the initial stage; α-S_8 can be further oxidized to $S_2O_3^{2-}$ in the later stage. Elemental S reacted with dissolved sulfide to form the intermediate polysulfide ions, including S_4^{2-} and S_5^{2-}. The concentration of dissolved Mn(II) in the filtrate was measured to be less than the detection limit, which may be due to the formation of $Mn(OH)_2$ precipitate.

Effect of temperature and pH

The initial rate of dissolved sulfide oxidation by birnessite, cryptomelane and todorokite follows a pseudo-first-order kinetics law at the initial stage (Qiu *et al*., 2011; Gao *et al*., 2015). The pseudo-first-order kinetics model for the redox reaction of dissolved sulfide and active manganese oxides has been derived in detail in previous studies. In the present work, manganite was used as the oxidant and the oxidation rate of dissolved sulfide was decreased. In the first 30 min of the experiment, the amount of manganese oxide minerals was excessive compared with that of HS^- and elemental S was the main oxidation product, which satisfied the requirement of the pseudo-first-order kinetics model. The influence of temperature and pH on the initial oxidation rate (k_{obs}, apparent rate constant) of dissolved sulfide by manganite was studied under nitrogen atmosphere in the present work.

The fitting curves of the pseudo-first-order kinetics model were used to compare the oxidation rates of HS^- by manganite with pH 12.0 at 20, 30, and 40ºC (Figure 3). The experimental data were well fitted by the pseudo-first-order kinetics law, and k_{obs} values were calculated to be 0.0408, 0.0678, and 0.1546 min^{-1} when the system temperature was controlled at 20, 30, and 40ºC, respectively. The initial apparent oxidation rate of dissolved sulfide increased significantly with increasing temperature. The apparent activation energy was calculated to be 50.7 kJ mol^{-1} from the Arrhenius equation (R^2 = 0.976), which was greater than that for the oxidation of dissolved sulfide by todorokite and birnessite in previous studies (Yao and Millero, 1993; Qiu *et al*., 2011; Gao *et al*., 2015), suggesting that the oxidation activity increased in the order of manganite < todorokite < birnessite because of their differences in crystal structures and Mn valence state under similar reaction conditions. The apparent activation energy may also be affected by reaction conditions such as pH and

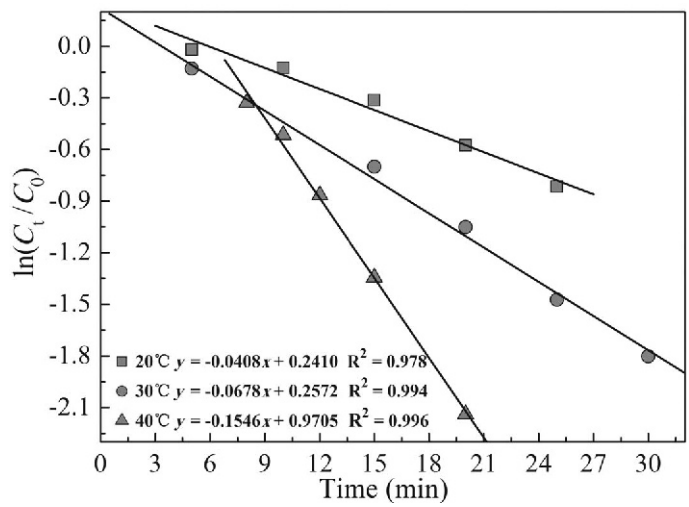

Figure 3. Fitting curves by the pseudo-first-order kinetics model at the initial stage of HS^- (400 mL, 200 mg L^{-1}) oxidation by γ-MnOOH (1.25 g L^{-1}) with pH 12.0 at different temperatures in nitrogen atmosphere. C_t and C_0 represented the concentrations of the dissolved sulfide at various times and at the initial stage, respectively.

https://doi.org/10.1346/CCMN.2017.064066 Published online by Cambridge University Press

chemical composition (Yao and Millero, 1993; Herszage and dos Santos Afonso, 2003).

As reported in previous studies, the initial pH had a minor effect on the reaction rate of sulfide oxidation due to the quick increase in pH (Luo *et al*., 2016). The effect of constant pH on the redox rate was further studied at the initial stage in this work, therefore, and the pseudo-first-order kinetics model was used to calculate the apparent rate constant k_{obs} (Figure 4). When the pH was fixed at 4.0, 6.0, 8.0, 10.0, and 12.0, k_{obs} values were set at 0.1051, 0.2008, 0.2133, 0.0967, and 0.0408 min^{-1}, respectively, and the largest k_{obs} was obtained at pH 8.0. The k_{obs} increased first and then decreased with increasing pH values in the reaction systems (Figure 4b), indicating a different reaction mechanism of sulfide oxidation in a wide pH range.

The pH affects the oxidation rate of sulfide primarily through adjusting the chemical speciation of dissolved sulfide and the surface sites on manganese dioxides (Yao and Millero, 1993). The chemical species of dissolved sulfide were influenced significantly by the concentration of H^+. The dissolved sulfides in the solution exist in different forms at different pH ranges, and the ionization equilibrium of dissolved sulfide in the reaction system is listed as follows (Rickard and Luther, 2006):

$$H_2S \xrightarrow{K_1} H^+ + HS^- \quad pK_1 = 6.88 \qquad (1)$$

As the pK_2 of H_2S_{aq} is assumed to be 14.15, the further ionization of HS^- to form S^{2-}_{aq} can be ignored over a wide pH range (Rickard and Luther, 2006), suggesting that H_2S and HS^- are the dominant species in acidic and alkaline aqueous systems. The fractions (α_i) of H_2S and HS^- could be calculated simply according to the dissociation constant as follows:

$$\alpha_{H_2S} = 1/(1 + K_1/[H^+]) \qquad (2)$$

$$\alpha_{HS^-} = 1/(1 + [H^+]/K_1) \qquad (3)$$

In the suspending liquid of manganite, the surface speciation is dependent on pH and can be expressed as the following ionization equilibrium (Zhu *et al*., 2009):

$$\equiv Mn^{III}OH \xrightarrow{K_1} \equiv Mn^{III}O^- + H^+ \quad pK_1' = 8.2 \qquad (4)$$

Dissociation constant

The fractions (α_j) of $\equiv Mn^{III}OH$ and $\equiv Mn^{III}O^-$ could also be calculated as follows:

$$\alpha_{\equiv Mn^{III}OH} = 1/(1 + K_1'/[H^+]) \qquad (5)$$

$$\alpha_{\equiv Mn^{III}O^-} = 1/(1 + [H^+]/K_1') \qquad (6)$$

During the oxidation processes, a surface complexation reaction occurred at first, and then electrons were transferred within the surface complex, and final oxidation products of sulfide and Mn(II) were released. The possible complex compounds have been characterized using various methods (Yao and Millero, 1993; Al-Farawati and van den Berg, 1999; Chadwell *et al*., 1999; Herszage and dos Santos Afonso, 2003; Rickard and Luther, 2006). Mn(II) sulfide complexes including $[Mn(HS)_2]^0$ and $[Mn(HS)]^+$ and polysulfide complexes have been detected by sulfide titration and cathodic stripping voltammetry (Al-Farawati and van den Berg, 1999; Chadwell *et al*., 1999; Rickard and Luther, 2006). Sulfide oxidation by Mn(IV) oxide proceeds *via* the formation of two different inner-sphere surface complexes $\equiv Mn^{IV}S^-$ and $\equiv Mn^{IV}SH$ according to the experimental results (Herszage and dos Santos Afonso, 2003). Similar sulfide complexes including $[\equiv MnOH][HS^-]$ and $[\equiv MnO^-][H_2S]$ were proposed to be the dominant intermediates of sulfide oxidation by δ-MnO_2 as indicated by curve fitting (Yao and Millero, 1993). The formation process of a precursor complex is usually affected by the relative distribution of different sites on manganese oxide surface and of sulfide in solution (Yao and Millero, 1993). In the present study, the possible complexation reactions in the first stage are presumed as follows:

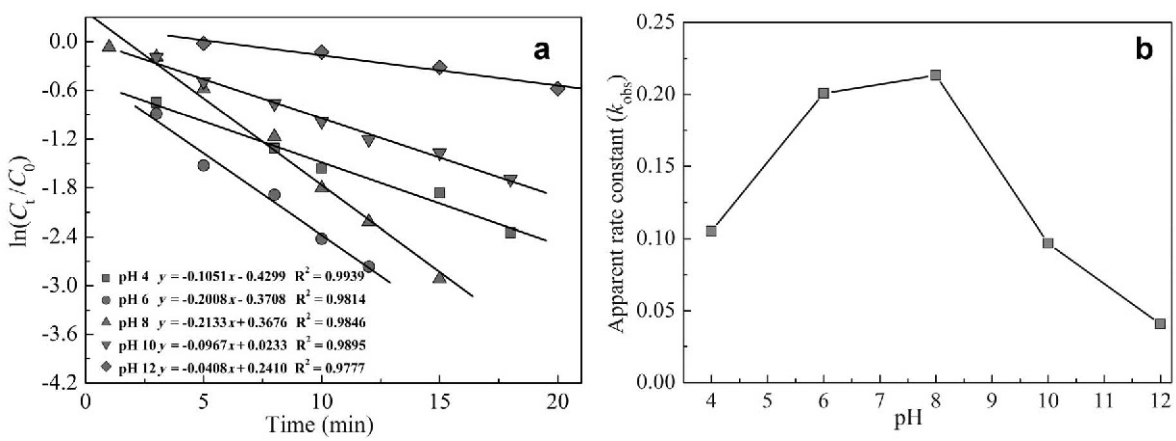

Figure 4. Fitting curves by pseudo-first-order kinetics model at the initial stage of HS^- (400 mL, 200 mg L^{-1}) oxidation by γ-MnOOH (1.25 g L^{-1}) with different pH (a), and the effect of pH on the apparent rate constant (b) at 20ºC in a nitrogen atmosphere.

https://doi.org/10.1346/CCMN.2017.064066 Published online by Cambridge University Press

$$\equiv Mn^{III}OH + H_2S \rightarrow \equiv Mn^{III}OSH + 2H^+ \quad (7)$$

$$\equiv Mn^{III}OH + HS^- \rightarrow \equiv Mn^{III}OSH + H^+ \quad (8)$$

$$\equiv Mn^{III}O^- + H_2S \rightarrow \equiv Mn^{III}OSH + H^+ \quad (9)$$

$$\equiv Mn^{III}O^- + HS^- \rightarrow \equiv Mn^{III}OSH \quad (10)$$

The degrees of ionization and chemical speciation for manganite and dissolved sulfides are affected significantly by pH according to equilibrium equations 1 and 4. The fraction products ($F = \alpha_i\alpha_j$) for the possible complexes were dependent on pH in the reaction system (Figure 5). When the pH was <6.0, the complexes existed mainly as $[\equiv Mn^{III}OH][H_2S]$, the proportion of which decreased with increasing pH. When the pH was >6.0, the proportion of $[\equiv Mn^{III}O^-][HS^-]$ increased with increasing pH. The fraction of $[\equiv Mn^{III}OH][HS^-]$ and $[\equiv Mn^{III}O^-][H_2S]$ increased at first and then decreased with increasing pH, and they had the greatest proportions at ~pH 8.0 and 7.5, respectively. The theoretical derivation and calculation above matched the experimental results, further indicating that $[\equiv Mn^{III}OH][HS^-]$ might be the main complex formed due to its proportion at pH 8.0. These results further indicated that surface-complexation reactions played an important role in controlling the initial oxidation rate of dissolved sulfide by manganite, and were affected significantly by pH.

Catalytic oxidation of dissolved sulfide by manganite in the presence of oxygen

Oxygen introduced from the atmosphere and rhizosphere usually participates in the oxidation of dissolved sulfides and Mn(II). $Mn(OH)_2$, which is formed from the reduction of Mn(IV) oxides, is oxidized to β-MnOOH in the presence of oxygen (Qiu *et al*., 2011). Metastable β-MnOOH can be transformed into γ-MnOOH (Stumm and Giovanoli, 1976). During the oxidation process of dissolved sulfide, the effect of oxygen on the redox rate and chemical stability of γ-MnOOH was further investigated in the present work.

The decreasing rate of dissolved sulfide concentration was reduced significantly when only oxygen participated in the oxidation of dissolved sulfide (Figure 6). The reaction rate increased when manganite was added to the oxygenated system. The decreasing rate of dissolved sulfide was less than that when only manganite was used as the oxidant in the reaction system, however. The oxidation capability of oxygen was much greater than that of manganite, suggesting that the apparent activation energy for the oxidation of dissolved sulfide by oxygen is less than that for the oxidation of HS^- by manganite (50.7 kJ mol^{-1}). This result further suggests that the oxidation rate of HS^- by oxygen is limited by the diffusion of dissolved sulfide onto the surface of manganite. In the present study, the rates of diffusion of dissolved sulfide and manganite together were greater than that of dissolved sulfide and oxygen molecules in aqueous solutions because the reaction rate was limited by diffusion processes for the low activation energy (Fersht, 2000; Gao *et al*., 2015). At the initial stage, the rate of dissolved sulfide oxidation by different oxidants followed the order oxygen < (manganite + oxygen) < manganite in the three reaction systems. Similar results were obtained when the strong oxidant todorokite was used (Gao *et al*., 2015).

The intermediates were further characterized to investigate the influence of oxygen on the oxidation processes of dissolved sulfide by γ-MnOOH (Figure 7a). $S_2O_3^{2-}$, SO_3^{2-}, and SO_4^{2-} were the main oxidation products when oxygen alone worked as the oxidant.

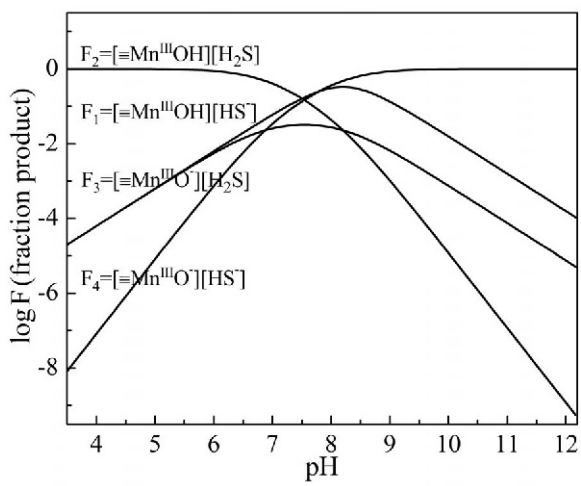

Figure 5. Effect of pH on the formation of precursor complexes for the reaction of HS^- (400 mL, 200 mg L^{-1}) and γ-MnOOH (1.25 g L^{-1}) at 20ºC in a nitrogen atmosphere.

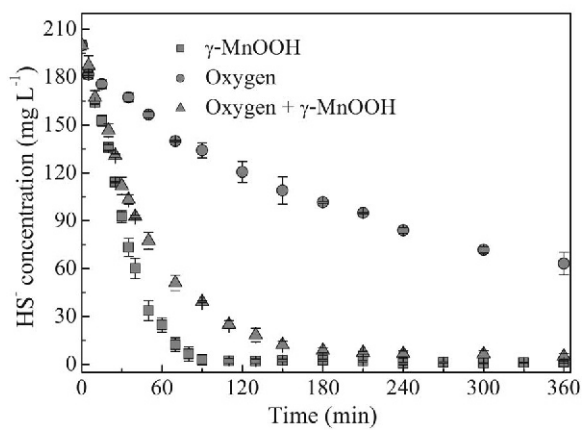

Figure 6. Concentrations of HS^- in reaction systems of sulfide (200 mg L^{-1}) oxidation by a number of oxidants at various times with pH 12.0 at 20ºC and 1.25 g L^{-1} of γ-MnOOH used in the experiment.

https://doi.org/10.1346/CCMN.2017.064066 Published online by Cambridge University Press

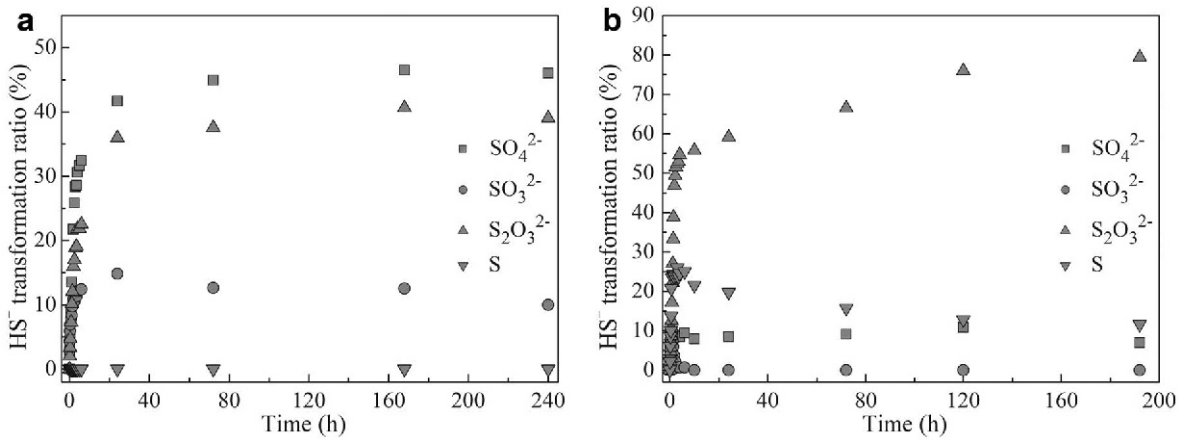

Figure 7. Transformation ratio from HS^- to intermediates for the oxidation by oxygen (a) and by γ-MnOOH (1.25 g L^{-1}) in oxygen atmosphere (b) for different times in an aqueous system with pH 12.0 at 20ºC.

Elemental sulfur was first formed and then oxidized to $S_2O_3^{2-}$ when both manganite and oxygen participated in the oxidation of dissolved sulfide for ~200 h of reaction (Figure 7b). The difference in the oxidation rate and oxidation products of dissolved sulfide by different oxidants was possibly due to the different redox mechanisms.

As reported by Hemmingsen (1992), the E_0 values for SO_4^{2-}/HS^-, SO_3^{2-}/HS^-, $S_2O_3^{2-}/HS^-$, and S/HS^- are 252, 368, 200, and −65 mV, respectively, the elemental sulfur and $S_2O_3^{2-}$ were, thus, formed easily owing to the difference in standard redox potentials. Due to the fact that oxygen showed greater oxidation activity than manganite, HS^- could be oxidized directly by oxygen to form $S_2O_3^{2-}$, SO_3^{2-}, and SO_4^{2-}. When oxygen was admitted into the reaction system of sulfide and manganite, dissolved sulfide would be complexed easily with manganite, and α-S_8 was formed rapidly at the initial stage. The reaction rate decreased owing to the restricted diffusion of oxygen with dissolved sulfide, though HS^- could be oxidized directly by oxygen to form $S_2O_3^{2-}$, SO_3^{2-}, and SO_4^{2-}. Dissolved oxygen was more likely to oxidize α-S_8 on the surface of manganese oxides because only a small amount of SO_3^{2-} and SO_4^{2-} was formed (Figure 7b). Some dissolved sulfide was oxidized by oxygen, resulting in a decrease in reactant concentration and the corresponding reaction rate with manganite.

The chemical stability of manganite was further studied during the redox process of dissolved sulfide and manganite (1.25 g L^{-1}) in the absence and presence of oxygen. In a nitrogen atmosphere (Figure 8a), the diffraction peaks of γ-MnOOH and $Mn(OH)_2$ were observed within the first 6 h, and α-S_8 diffraction peaks also appeared at 6 h and increased over time, implying an increase in the α-S_8 content in solid products. Mn_3O_4 (JCPDS card ID: 16-0350) was observed owing to the further oxidation of $Mn(OH)_2$ in air. After filtration separation, wet intermediates on a filter membrane were exposed to air during the

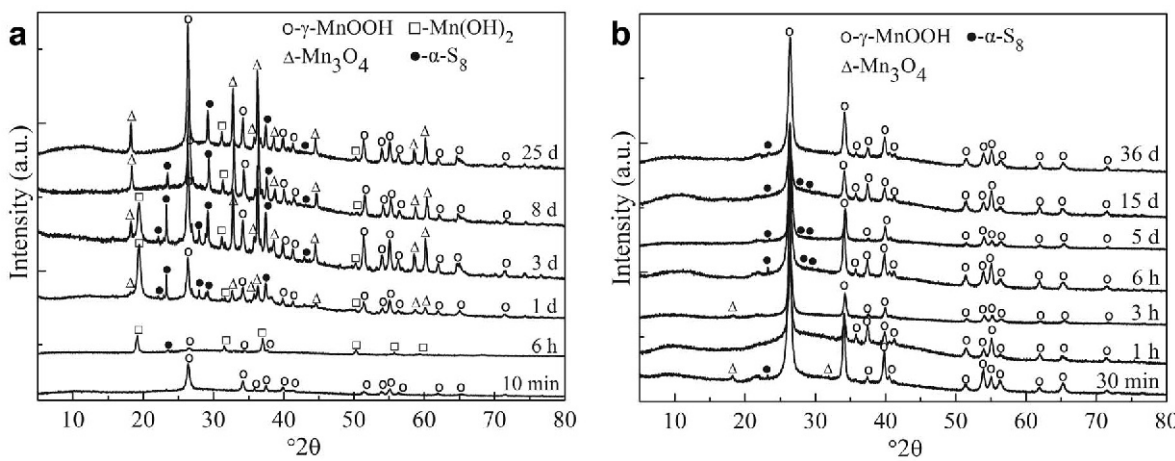

Figure 8. XRD patterns of solid products of the redox reaction of γ-MnOOH (1.25 g L^{-1}) and HS^- (400 mL, 200 mg L^{-1}) in nitrogen (a) and oxygen (b) atmosphere with pH 12.0 at 20ºC.

https://doi.org/10.1346/CCMN.2017.064066 Published online by Cambridge University Press

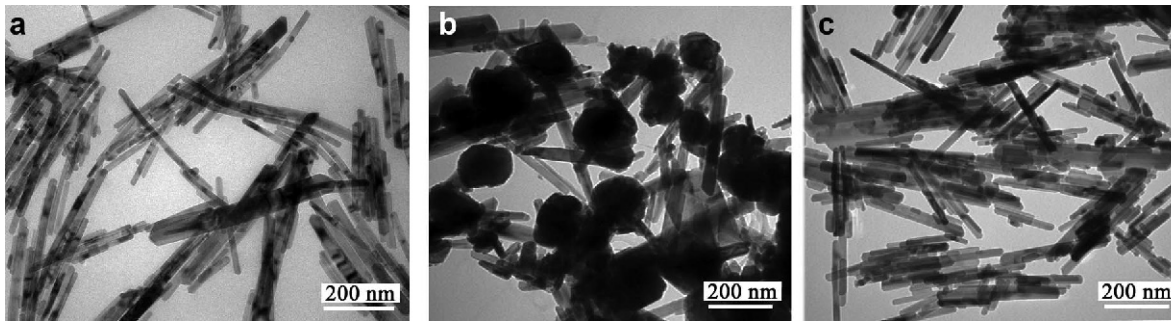

Figure 9. TEM images of synthesized γ-MnOOH (a) and of solid products from the reaction system of γ-MnOOH (1.25 g L^{-1}) and HS^- (400 mL, 200 mg L^{-1}) with pH 12.0 at 20ºC for 25 days in nitrogen atmosphere (b) and for 36 days in oxygen atmosphere (c).

subsequent XRD test, which facilitated the further oxidation of $Mn(OH)_2$ to Mn_3O_4 by oxygen in air (Qiu *et al*., 2011; Gao *et al*., 2015). When oxygen was introduced into the reaction system above, only a very small amount of Mn_3O_4 was formed at the initial stage which then disappeared after 3 h of reaction owing to its re-oxidation to form manganite in an oxygenated aqueous system (Figure 8b). Elemental sulfur was formed as indicated by the increase in the intensity of diffraction peaks in the first 6 h, and the diffraction peak intensity attenuated after 5 days due to the further oxidation to $S_2O_3^{2-}$ by oxygen. The presence of oxygen facilitated the rapid transformation from α-S_8 to $S_2O_3^{2-}$ and the re-oxidation of Mn_3O_4 to manganite (Qiu *et al*., 2011; Gao *et al*., 2015). Manganite can, therefore, definitely be considered to have excellent catalytic activity for the oxidation of dissolved sulfide by oxygen.

The catalytic stability of manganite was further confirmed by TEM analysis. Manganite had the rod-like nanostructures with rod lengths ranging from 200 to 500 nm (Figure 9a). In a nitrogen atmosphere, the typical rod-like γ-MnOOH particles were collapsed with the presence of polyhedral particles owing to the formation of Mn_3O_4 from the oxidation of $Mn(OH)_2$ after 25 days of reaction (Figure 9b). In an oxygen atmosphere, no other solid products were observed after 36 days of reaction, however, and the rod lengths of manganite were reduced, which was possibly due to the re-oxidation of Mn_3O_4 (Figure 9c). During a similar redox process, the crystal structure of todorokite was collapsed significantly because of its greater oxidation activity (Gao *et al*., 2015). Manganite can be formed readily from the oxidation of Mn_3O_4 precipitate by oxygen in soil environments (Kirillov *et al*., 2009). In the present study, Mn_3O_4 precipitate formed from the reduction of manganite by sulfide could be reoxidized rapidly to manganite by oxygen. During the oxidation processes of dissolved sulfide by oxygen, manganite facilitated the oxidation of dissolved sulfide to $S_2O_3^{2-}$, and the crystal structure was maintained for more than a month, exhibiting excellent catalytic activity and chemical stability.

CONCLUSIONS

The presence of manganite accelerated the oxidation of sulfide in aqueous systems under both nitrogen and oxygen atmospheres, and affected the migration and transformation of dissolved sulfide. Sulfide was oxidized by manganite to form elemental sulfur, which was further transformed slowly into $S_2O_3^{2-}$ in a nitrogen atmosphere. Polysulfide ions were an important intermediate during the redox process. The oxidation rate of dissolved sulfide increased with increasing temperature, and decreased with the participation of oxygen. The dissolved sulfide oxidation rate increased at first and then decreased with increasing pH from 4.0 to 12.0, and the maximum oxidation rate was achieved at a pH of ~8.0 owing to the formation of the main complex $[\equiv Mn^{III}OH][HS^-]$. Surface complexation reactions played an important role in controlling the initial oxidation rate of dissolved sulfide by manganite and were affected significantly by pH. Manganite exhibited excellent catalytic activity and stability for the rapid oxidation of dissolved sulfide to $S_2O_3^{2-}$ by oxygen.

ACKNOWLEDGMENTS

The present study was supported by the National Natural Science Foundation of China (Grant Nos: 41171375, 41571228, 41425006, and 41330852), the Fok Ying-Tong Education Foundation (No. 141024), the Natural Science Foundation of the Hubei Province of China (No. 2014CFA016), and the Fundamental Research Funds for the Central Universities (Program No.: 2662015JQ002). The authors acknowledge Dr Le Ge at the Chemical Sciences and Engineering Division at Argonne National Laboratory for helpful suggestions.

REFERENCES

Al-Farawati, R. and van den Berg, C.M.G. (1999) Metal–sulfide complexation in seawater. *Marine Chemistry*, **63**, 331–352.

Aller, R.C. and Rude, P.D. (1988) Complete oxidation of solid phase sulfides by manganese and bacteria in anoxic marine sediments. *Geochimica et Cosmochimica Acta*, **52**, 751–765.

Caldwell, W.E. and Krauskopf, F.C. (1929) Reduction reactions with calcium hydride. I. Rapid determination of sulfur

https://doi.org/10.1346/CCMN.2017.064066 Published online by Cambridge University Press

in insoluble sulfate. *Journal of the American Chemical Society*, **51**, 2936–2942.

Chadwell, S.J., Rickard, D., and Luther III, G.W. (1999) Electrochemical evidence for pentasulfide complexes with Mn^{2+}, Fe^{2+}, Co^{2+}, Ni^{2+}, Cu^{2+} and Zn^{2+}. *Aquatic Geochemistry*, **5**, 29–57.

Duckworth, O.W. and Sposito, G. (2005) Siderophore-manganese(III) interactions II. Manganite dissolution promoted by desferrioxamine B. *Environmental Science & Technology*, **39**, 6045–6051.

Fersht, A.R. (2000) Transition-state structure as a unifying basis in protein-folding mechanisms: Contact order, chain topology stability and the extended nucleus mechanism. *Proceedings of the National Academy of Sciences*, **97**, 1525–1529.

Filpponen, I., Guerra, A., Hai, A., Lucia, L.A., and Argyropoulos, D.S. (2006) Spectral monitoring of the formation and degradation of polysulfide ions in alkaline conditions. *Industrial & Engineering Chemistry Research*, **45**, 7388–7392.

Gao, T.Y., Shi, Y., Liu, F., Zhang, Y.S., Feng, X.H., Tan, W.F., and Qiu, G.H. (2015) Oxidation process of dissolvable sulfide by synthesized todorokite in aqueous systems. *Journal of Hazardous Materials*, **290**, 106–116.

Giovanoli, R. and Leuenberger, U. (1969) Über die oxydation von manganoxidhydroxid. *Helvetica Chimica Acta*, **52**, 2333–2347.

Golden, D.C., Chen, C.C., and Dixon, J.B. (1987) Transformation of birnessite to buserite, todorokite, and manganite under mild hydrothermal treatment. *Clays and Clay Minerals*, **35**, 271–280.

Hem, J.D. (1981) Rates of manganese oxidation in aqueous systems. *Geochimica et Cosmochimica Acta*, **45**, 1369–1374.

Hemmingsen, T. (1992) The electrochemical reaction of sulphur-oxygen compounds – Part I. A review of literature on the electrochemical properties of sulphur/sulphur-oxygen compounds. *Electrochimica Acta*, **37**, 2775–2784.

Herszage, J. and dos Santos Afonso, M. (2003) Mechanism of hydrogen sulfide oxidation by manganese(IV) oxide in aqueous solutions. *Langmuir*, **19**, 9684–9692.

Hoffmann, M.R. (1977) Kinetics and mechanism of oxidation of hydrogen sulfide by hydrogen peroxide in acidic solution. *Environmental Science & Technology*, **11**, 61–66.

Johnson, D.B. and Hallberg, K.B. (2003) The microbiology of acidic mine waters. *Research in Microbiology*, **154**, 466–473.

Kamyshny, A., Jr., Goifman, A., Gun, J., Rizkov, D., and Lev, O. (2004) Equilibrium distribution of polysulfide ions in aqueous solutions at 25°C: A new approach for the study of polysulfides' equilibria. *Environmental Science & Technology*, **38**, 6633–6644.

Kirillov, S.A., Aleksandrova, V.S., Lisnycha, T.V., Dzanashvili, D.I., Khainakov, S.A., García, J.R., Visloguzova, N.M., and Pendelyuk, O.I. (2009) Oxidation of synthetic hausmannite (Mn_3O_4) to manganite (MnOOH). *Journal of Molecular Structure*, **928**, 89–94.

Li, H., Ye, Z.H., Wei, Z.J., and Wong, M.H. (2011) Root porosity and radial oxygen loss related to arsenic tolerance and uptake in wetland plants. *Environmental Pollution*, **159**, 30–37.

Lippa, K.A. and Roberts, L. (2002) Nucleophilic aromatic substitution reactions of chloroazines with bisulfide (HS^-) and polysulfides (S_n^{2-}). *Environmental Science & Technology*, **36**, 2008–2018.

Liu, C., Zhang, L., Li, F., Wang, Y., Gao, Y., Li, X., Cao, W., Feng, C., Dong, J., and Sun, L. (2009) Dependence of sulfadiazine oxidative degradation on physicochemical properties of manganese dioxides. *Industrial & Engineering Chemistry Research*, **48**, 10408–10413.

Luo, Y., Li, S., Tan, W.F., Liu, F., Cai, C.F., and Qiu, G.H. (2016) Oxidation process of dissolvable sulfide by manganite sulfide and its influence factors. *Environmental Science*, **37**, 1539–1545 (in Chinese).

Luo, Y., Shen, Y.G., Liu, L.H., Hong, J., Qiu, G.H., Tan, W.F., and Liu, F. (2017) In situ detection of intermediates from the interaction of dissolved sulfide and manganese oxides with a platinum electrode in aqueous systems. *Environmental Science*, **14**, 178–187.

Möckel, H.J. (1984) Retention of sulphur and sulphur organics in reversed-phase liquid chromatography. *Journal of Chromatography A*, **317**, 589–614.

Mongelli, G., Sinisi, R., Mameli, P., and Oggiano, G. (2015) Ce anomalies and trace element distribution in Sardinian lithiophorite-rich Mn concretions. *Journal of Geochemical Exploration*, **153**, 88–96.

Murray, J.W., Dillard, J.G., Giovanoli, R., Moers, H., and Stumm, W. (1985) Oxidation of Mn (II): Initial mineralogy, oxidation state and ageing. *Geochimica et Cosmochimica Acta*, **49**, 463–470.

Nico, P.S. and Zasoski, R.J. (2001) Mn(III) center availability as a rate controlling factor in the oxidation of phenol and sulfide on δ-MnO_2. *Environmental Science & Technology*, **35**, 3338–3343.

Qiu, G.H., Li, Q., Yu, Y., Feng, X.H., Tan, W.F., and Liu, F. (2011) Oxidation behavior and kinetics of sulfide by synthesized manganese oxide minerals. *Journal of Soils and Sediments*, **11**, 1323–1333.

Rickard, D.T. (1974) Kinetics and mechanism of the sulfidation of goethite. *American Journal of Science*, **274**, 941–952.

Rickard, D. and Luther III, G.W. (2006) Metal sulfide complexes and clusters. Pp. 421–504 in: *Sulfide Mineralogy and Geochemistry* (D.J. Vaughan, editor). Reviews in Mineralogy and Geochemistry, **61**, Mineralogical Society of America, Chantilly, Virginia, USA.

Schippers, A. and Jørgensen, B.B. (2001) Oxidation of pyrite and iron sulfide by manganese dioxide in marine sediments. *Geochimica et Cosmochimica Acta*, **65**, 915–922.

Schippers, A., Jozsa, P., and Sand, W. (1996) Sulfur chemistry in bacterial leaching of pyrite. *Applied and Environmental Microbiology*, **62**, 3424–3431.

Shamsul Haque, K.M., Eberbach, P.L., Weston, L.A., Dyall-Smith, M., and Howitt, J.A. (2015) Pore Mn^{2+} dynamics of the rhizosphere of flooded and non-flooded rice during a long wet and drying phase in two rice growing soils. *Chemosphere*, **134**, 16–24.

Stumm, W. and Giovanoli, R. (1976) Nature of particulate manganese in simulated lake waters. *Chimia*, **30**, 423–425.

Toner, B., Manceau, A., Webb, S.M., and Sposito, G. (2006) Zinc sorption to biogenic hexagonal birnessite particles within a hydrated bacterial biofilm. *Geochimica et Cosmochimica Acta*, **70**, 27–43.

Tu, S., Racz, G.J., and Goh, T.B. (1994) Transformations of synthetic birnessite as affected by pH and manganese concentration. *Clays and Clay Minerals*, **42**, 321–330.

Walker, J.R. and Hayes, T.H. (1990) Reaction scheme for the oxidation of As (III) to As (V) by birnessite. *Clays and Clay Minerals*, **38**, 549–555.

Weaver, R.M., Hochella, M.F., and Ilton, E.S. (2002) Dynamic processes occurring at the Cr^{III}_{aq}-manganite (γ-MnOOH) interface: simultaneous adsorption, microprecipitation, oxidation/reduction, and dissolution. *Geochimica et Cosmochimica Acta*, **66**, 4119–4132.

Xu, X.J., Chen, C., Wang, A.J., Guo, W.Q., Zhou, X., Lee, D.-J., Ren, N.Q., and Chang, J.-S. (2014) Simultaneous removal of sulfide, nitrate and acetate under denitrifying sulfide

removal conditions: Modeling and experimental validation. *Journal of Hazardous Materials*, **264**, 16–24.

Yao, W.S. and Millero, F.J. (1993) The rate of sulfide oxidation by δMnO_2 in seawater. *Geochimica et Cosmochimica Acta*, **57**, 3359–3365.

Zhang, C., Ge, Y., Yao, H., Chen, X., and Hu, M. (2012) Iron oxidation-reduction and its impacts on cadmium bioavailability in paddy soils: a review. *Frontiers of Environmental Science & Engineering*, **6**, 509–517.

Zhu, M.Q., Paul, K.W., Kubicki, J.D., and Sparks, D.L. (2009) Quantum chemical study of arsenic(III, V) adsorption on Mn-oxides: Implications for arsenic(III) oxidation. *Environmental Science & Technology*, **43**, 6655–6661.

(*Received 30 June 2017; revised 13 September 2017; Ms. 1186; AE: Luyi Sun*)